

Phase behavior of HFCs+HFCs, HFCs+Propane, HFCs+Propylene system using nonrandom lattice fluid theory

Sun Jin Lee, Hyun Sang Jin, Youn Woo Lee, Jong Sung Lim and Ki-Pung Yoo

Hoseo University, Asan City, Korea

09:20~10:50

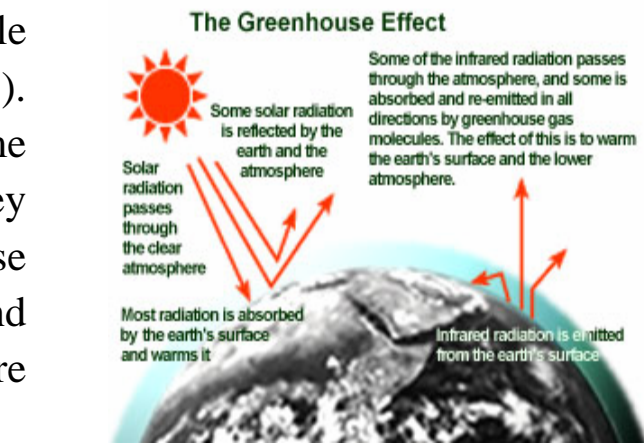
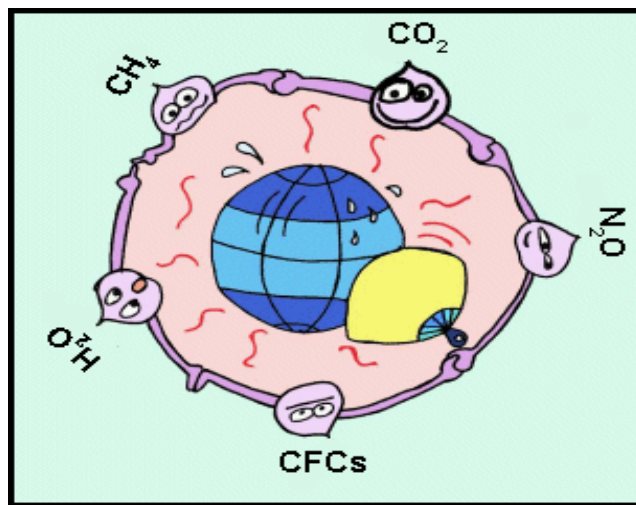
10. 29, 2004

Dept of Chem&Bio., Sogang University

KIST, Seoul National University

Introduction

Much effort has been made to find the suitable replacement for chlorofluorocarbons (CFCs). Initial CFC alternatives included some hydrochlorofluorocarbons (HCFCs) but they will be also phased out internationally because their ozone depletion potentials (ODPs) and global warming potentials (GWPs) are significant though less than those of CFCs.



Hydrofluorocarbons (HFCs) synthetic refrigerants Which have zero ODPs were proposed as promising replacements for CFCs and HCFCs. Unfortunately, HFCs have been included in the basket of green house gases to be regulated by Kyoto Protocol 1997 because their GWPs are several 1000 times higher than CO₂.

Purpose of research

- Vapor–liquid equilibrium (VLE) data were measured for HFCs + HFCs, HFCs + Propane, HFCs + Propylene system at various isotherms(263.15 – 323.15 K).
- The measure data were correlated by the nonrandom lattice Fluid (NLF) equation of state.
- For the measured and calculated data of HFCs + Propylene, HFCs + HFCs, HFCs + Propane systems, the relative accuracy of the data was discussed.



1) NLF EOS

$$P = -\frac{1}{v_H} \left(\frac{\partial \beta A^c}{\partial N_i} \right)_{T, N_j} = -\frac{1}{v_H \beta} \left(\frac{\partial A^c \beta}{\partial N_0} \right)_{T, N_i}$$

$$\frac{Pv_H}{RT} = \frac{z}{2} \ln \left[- + \left(\frac{q_M}{r_M} - 1 \right) \rho \right] - \ln(1 - \rho) + \rho \frac{l_M}{r_M} - \frac{z\beta}{2} \varepsilon_M \theta^2$$

$$\varepsilon_M = \frac{1}{\theta^2} \left[\sum_i \sum_j \theta_i \theta_j \varepsilon_{ij} + \left(\frac{\beta}{2} \right) \sum_i \sum_j \sum_k \sum_l \theta_i \theta_j \theta_k \theta_l \varepsilon_{ij} (\varepsilon_{ij} + 3\varepsilon_{kl} - 2\varepsilon_{ik} - 2\varepsilon_{jk}) \right]$$

2) NLF Chemical Potential

$$\frac{\mu_i}{N_A RT} = \left(\frac{\partial \beta A^c}{\partial N_i} \right)_{T, N_j} + \frac{r_i v_H P}{kT}$$

$$\frac{\mu_i}{RT} = (r_i + l_i) \ln \left[1 + \ln \left(\frac{q_M}{r_M} - 1 \right) \rho \right] - r_i \ln(1 - \rho) + \ln \left(\frac{\theta_i}{q_i} \right)$$

$$+ \left(\frac{z\beta}{2} \right) q_i \varepsilon_M \theta^2 \left[1 - \frac{r_i}{q_i} - \frac{2 \sum \theta_k \varepsilon_{ik} + \beta \sum \sum \sum \theta_i \theta_j \theta_k \varepsilon_{ij} (\varepsilon_{ij} + 2\varepsilon_{kl} - 2\varepsilon_{jk} - \varepsilon_{ik})}{\varepsilon_M \theta^2} \right]$$



● Pure parameter

- **volume parameter** $\triangleright V^*$
- **energy parameter** $\triangleright e_{ii}$ ***with z = 10, V_H = 9.75cm³mol⁻¹***

$$\varepsilon_{ii} / k = \left(\varepsilon_i^A / k \right) + \left(\varepsilon_{ii}^B / k \right) (T - T_0) + \left(\varepsilon_{ii}^C / k \right) \left(T \ln \frac{T_0}{T} + T - T_0 \right) \text{ After, Kehiaian(1978)}$$

$$\varepsilon_{ii}(T_r = 0.7) = 81.1297 [1 - \exp(-59.1693 \cdot V_{vdW})] + 56.2642 [1 - \exp(-6.4252 \cdot V_{vdW})]$$

$$r_i = r_i^A + r_i^B (T - T_0) + r_i^C \left(T \ln \frac{T_0}{T} + T - T_0 \right) \quad T_0 = 298.15 K = 25 C$$

$$r_i(T_r = 0.7) = 2.1785 + 133.8542 \cdot V_{vdW} (m^3 mol^{-1})$$

● Binary interaction parameter : λ_{ij}

$$\varepsilon_{ij} = (\varepsilon_{ii} \varepsilon_{jj})^{1/2} (1 - \lambda_{ij})$$



Result 1

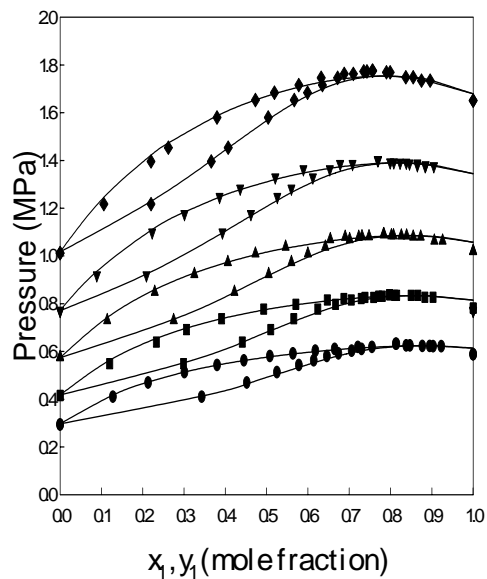


Figure 1. P-x-y diagram of the R1270 + HFC-134a system :
(-)calibration with NLF EOS;
Experimental data at
(●)273.15K; (■)283.15K;
(▲)293.15K; (▼)303.15K;
(◆)313.15K

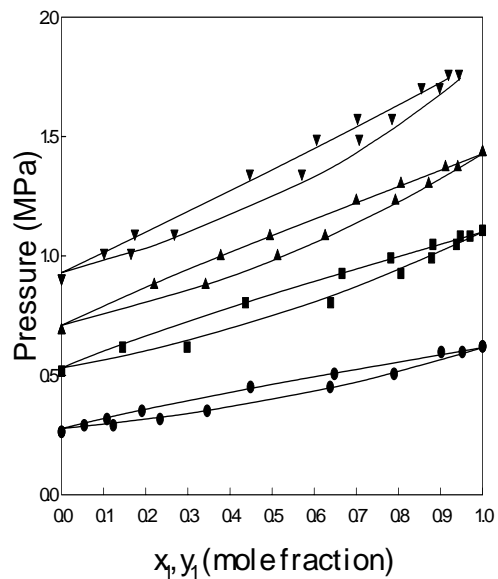


Figure 2. P-x-y diagram of the HFC143a + HFC-152a system:
(-)calibration with NLF EOS;
Experimental data at
(●)273.15K; (■)293.15K;
(▲)303.15K; (▼)313.15K

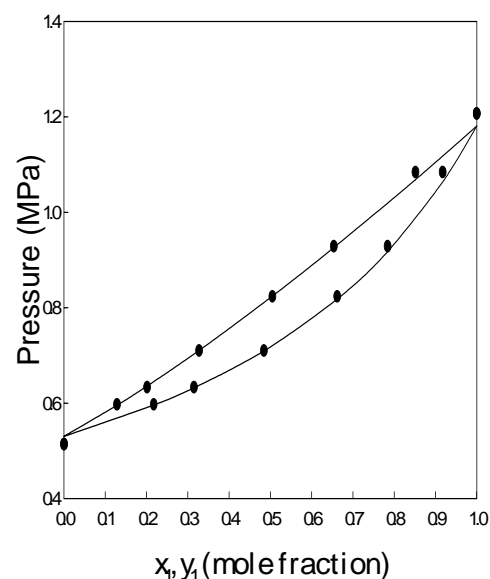


Figure 3. P-x-y diagram of the HFC143a + HFC-152a system:
(-)calibration with NLF EOS;
Experimental data at
(●)293.15K



Result 2

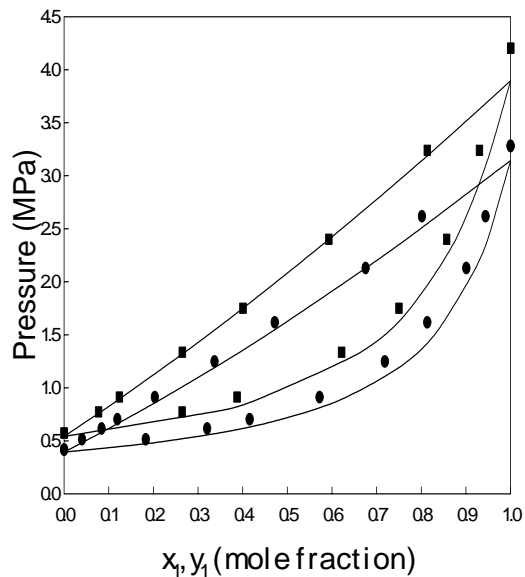


Figure 4. P-x-y diagram of the HFC23 + HFC-32 system:
(-)calibration with NLF EOS;
Experimental data at
(●)283.15K; (■) 293.15K

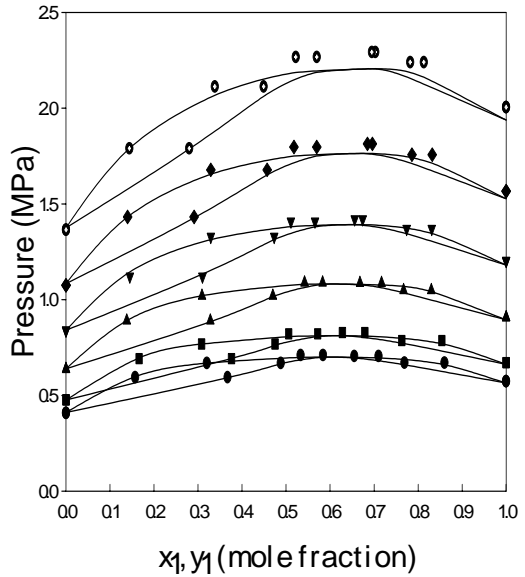


Figure 5. P-x-y diagram of the HFC-125 + Propane system:
(-)calibration with NLF EOS;
Experimental data at
(●)268.15K;(■)273.15K;
(▲)283.15K;(▼)293.15K;
(◆)303.15K;(✳)318.15K

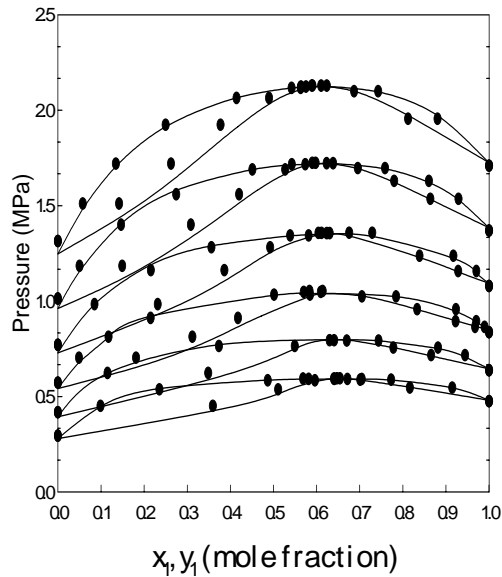


Figure 6. P-x-y diagram of the HFC-134a + Propane system:
(-)calibration with NLF EOS;
Experimental data at
(●)273.15K; (■)283.15K;
(▲)293.15K; (▼)303.15K;
(◆)313.15K; (✳)323.15K



Result 3

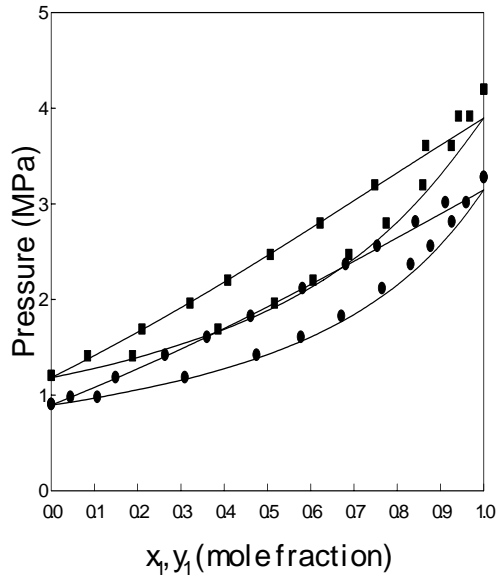


Figure 7. P-x-y diagram of the HFC-125 + HFC-23 system:
(-)calibration with NLF EOS;
Experimental data at
(●)283.15K; (■)293.15K

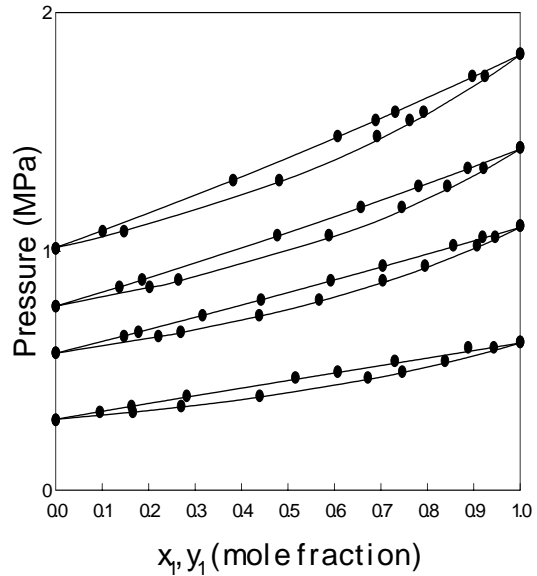


Figure 8. P-x-y diagram of the HFC143a + HFC-134a system:
(-)calibration with NLF EOS;
Experimental data at
(●)273.15K; (■)293.15K;
(▲)303.15K; (▼)313.15K

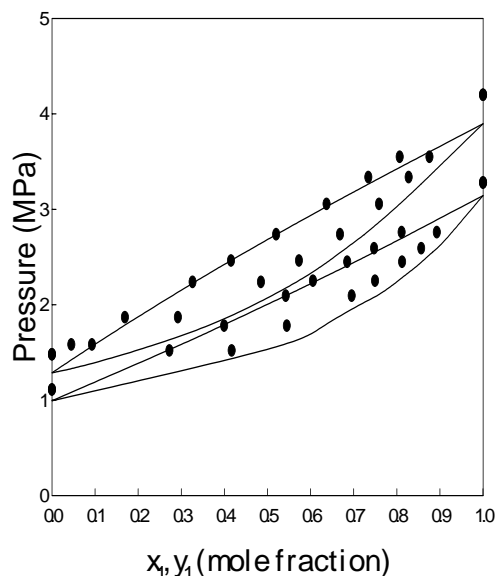


Figure 9. P-x-y diagram of the HFC23 + HFC-32 system:
(-)calibration with NLF EOS;
Experimental data at
(●)283.15K; (■)293.15K



Thermodynamic properties

	Chemical formula	T _C (K)	P _C (Mpa)	ω
HFC-32	CH ₂ F ₂	351.6	3.65	0.183
HFC-23	CHF ₃	299.1	4.84	0.263
HFC-125		339.3	6.63	0.304
HFC-152a	C ₂ H ₄ F ₂	386.6	4.50	0.256
HFC-143a	CH ₃ CH ₂ F	374.2	4.06	0.327
HFC-134a	C ₂ H ₂ F ₄	374.3	4.07	0.327
HC-290	C ₃ H ₈	369.8	4.25	0.152
R-1270	CH ₂ CHCH ₃	365.6	4.67	0.141



Average absolute deviation 1

T(K)	R-1270 + HFC-134a		HFC-143a + HFC-152a		HFC-125 + HFC-152a	
	AAD-y	AAD-P(%)	AAD-y	AAD-P(%)	AAD-y	AAD-P(%)
273.15	0.02272	0.78095	0.012802	1.94680	-	-
283.15	0.02489	0.86336	-	-	-	-
293.15	0.01924	0.81054	0.039439	0.93410	0.010855	0.974860
303.15	0.04136	0.57965	0.010199	0.73217	-	-
313.15	0.02097	0.91950	0.008943	1.75179	-	-

T(K)	HFC-143a + propane		T(K)	HFC-125+ propane	
	AAD-y	AAD-P(%)		AAD-y	AAD-P(%)
268.15	0.01866	0.41340	268.15	0.00843	1.06276
278.15	0.00693	0.41402	273.15	0.01172	1.17169
288.15	0.00448	0.38409	283.15	0.00913	0.58694
298.15	0.00245	0.33053	293.15	0.00693	1.56662
308.15	0.00519	0.23487	303.15	0.00598	1.84992
318.15	0.00563	0.29030	313.15	0.00634	2.52452



Average absolute deviation 2

T(K)	HFC-134a + propane		HFC-125 +HFC-23		HFC-143a +HFC-134a	
	AAD-y	AAD-P(%)	AAD-y	AAD-P(%)	AAD-y	AAD-P(%)
273.15	0.02493	0.89844	-	-	0.01465	1.19023
283.15	0.03128	1.29838	0.010796	1.41636	-	-
293.15	0.04711	1.31673	0.022819	2.03558	0.01642	0.33285
303.15	0.04473	1.31535	-	-	0.01653	0.23974
313.15	0.04457	0.98845	-	-	0.01460	0.21418
323.15	0.05085	0.91445	-	-	-	-

T(K)	HFC-23+ HFC-32		HFC-23 + HFC-134a	
	AAD-y	AAD-P(%)	AAD-y	AAD-P(%)
283.15	0.067187	2.66065	0.047020	4.85525
293.15	0.097226	4.59514	0.058160	2.61614

$$AAD - P(\%) = \frac{1}{N} \sum_{i=1}^N \left(\frac{\Delta P_i}{P_{exp, i}} \times 100 \right)$$

$$AAD - y = \frac{1}{N} \sum_{i=1}^N (\Delta y_i)$$



Conclusion

- The VLE of HFCs + HFCs, HFCs + Propane, HFCs + Propylene system used the NLF equation of state.
- The vapor-liquid equilibrium between measured and calculated values (AAD-P(%)) for HFCs + HFCs, HFCs + Propane, HFCs + Propylene from 263.15K to 323.15K and the deviations were less than 1.51%.
- In this temperature, azeotropic behavior has been found in HFCs + Propane, HFCs + Propylene systems.

